

# Chapter 15

## A Review and Some New Issues on the Theory of the H/V Technique for Ambient Vibrations

Enrico Lunedei and Peter Malischewsky

**Abstract** In spite of the Horizontal-to-Vertical Spectral Ratio (HVSR or H/V) technique obtained by the ambient vibrations is a very popular tool, a full theoretical explanation of it has been not reached yet. A short *excursus* is here presented on the theoretical models explaining the H/V spectral ratio that have been development in last decades. It leads to the present two main research lines: one aims at describing the H/V curve by taking in account the whole ambient-vibration wavefield, and another just studies the Rayleigh ellipticity. For the first theoretical branch, a comparison between the most recent two models of the ambient-vibration wavefield is presented, which are the Distributed Surface Sources (DSS) one and the Diffuse Field Approach (DFA). A mention is done of the current developments of these models and of the use of the DSS for comparing the H/V spectral ratio definitions present in literature. For the second research branch, some insights about the connection between the so-called osculation points of the Rayleigh dispersion curves and the behaviour of the H/V curve are discussed.

### 15.1 Introduction

The Horizontal-to-Vertical Spectral Ratio (HVSR or H/V) technique is a way to retrieve information about the shallow-subsoil seismic properties (which are of engineering interest) by single-station measurements carried out on the Earth's surface. This method is widely used in seismic exploration as a tool for a quick detection and evaluation of seismic-amplification effects in terms of S-wave resonance frequency as well as for constraining the elastic properties of the shallow geological structure (usually under the assumption of horizontally layered

---

E. Lunedei, PhD (✉)

Dipartimento di Scienze Fisiche, della Terra e dell'Ambiente, Università di Siena, Siena, Italy  
e-mail: [lunedei@unisi.it](mailto:lunedei@unisi.it)

P. Malischewsky

Institute of Geosciences, Friedrich-Schiller University Jena, Jena, Germany  
e-mail: [p.mali@uni-jena.de](mailto:p.mali@uni-jena.de)

© The Author(s) 2015

A. Ansal (ed.), *Perspectives on European Earthquake Engineering and Seismology*,  
Geotechnical, Geological and Earthquake Engineering 39,  
DOI 10.1007/978-3-319-16964-4\_15

371

medium). Nevertheless, some controversial aspects about the exact physical interpretation of the outcome provided by this technique (the H/V curve) remain. Most of them are related with the nature of the ambient-vibration wavefield and of its sources. These differences in the H/V curve modelling might have consequences in the results of inversion procedures used to infer the subsoil stratigraphical profile from experimental measurements.

From the experimental point of view, this technique requires a three-component ground-motion acquisition and consists in performing the ratio between its horizontal and vertical Fourier spectrum, properly averaged on an adequate sample. This ratio, which is a function of the frequency, is called the H/V (or HVSR) curve (or function). The ratio is usually computed by using ground-motion velocity spectra, but displacement or acceleration spectra can be used as well. The two horizontal motion components can be combined in different ways (*vide infra*).

In order to fully exploit the H/V curve to constrain subsoil seismic-properties, some theoretical model is necessary to link the H/V pattern to the mechanical properties of geological bodies under the measuring site. As the H/V refers to ambient vibrations, any model of H/V is also a model, explicit or tacit, of the ambient-vibration wavefield, and thus it should be consistent with the other findings about the ambient-vibration wavefield, and not just gives a plausible way to reproduce the H/V curve only.

In next section, a short *excursus* on the history of the H/V theoretical explanations is presented. The most part of the proposed models, which are the sole ones considered in this review, describes the Earth as 1D medium, *i.e.*, a stack of homogeneous and isotropic horizontal layers overlying an half-space with the same characteristics. They are the models widely used, while 2D and 3D ones, which are very cumbersome under many aspects, have been playing, so far, a minor role, being their use limited to specific problems (see, *e.g.*, Bonnefoy-Claudet et al. 2004).

## 15.2 A Short Review on the H/V Theory

Kanai and Tanaka (1961) use the ambient-vibration horizontal-motion spectra to infer seismic subsoil properties, even if they already recognize that the ambient-vibration features depend on both site mechanical-properties and ambient-vibration sources' characteristics. Other authors, however, note that ambient-vibration spectra often reflect more the sources' characteristics rather than the subsoil ones (cf. Tokimatsu 1997).

### 15.2.1 The H/V Origins: Body-Wave Based Theories

Nakamura and Ueno (1986), after the Nogoshi and Igarashi's (1971) work, widespread the H/V technique, in which the effects of the source are supposed to be minimized normalizing the horizontal ground-motion spectral component by the vertical one. In the first theoretical explanation proposed by Nakamura (1989), ambient vibrations are supposed to be composed by S and Rayleigh waves, but the effect of these last ones is "eliminated" by considering the H/V spectral ratio

$$HV(\omega) \equiv \frac{A_{H,surface}^{FW}(\omega)}{A_{V,surface}^{FW}(\omega)}, \quad (15.1)$$

where  $A_{H,surface}^{FW}$  and  $A_{V,surface}^{FW}$  are the total (hereafter, *FW* means full-wavefield) spectral amplitudes of the horizontal and, respectively, vertical ground-motion at the Earth's surface, and  $\omega$  is the angular frequency. By assuming that the analogous H/V spectral ratio computed at the bedrock is approximately unitary and that the vertical motion does not undergo any stratigraphical amplification, the Author shows that the ratio in Eq. 15.1 equals the horizontal soil transfer-function normalized by the vertical one. In this view, the H/V ratio directly would represent the amplification phenomena affecting the horizontal ground-motion. After some criticisms, Nakamura modified his interpretation of H/V spectral ratio. As expressed in Nakamura (2000), by considering the ambient-vibration wavefield composed by just vertically incident P and S waves along with Rayleigh waves, he separates these components by writing the horizontal and vertical spectral ground-motion amplitudes at the Earth's surface as

$$\begin{aligned} A_{\delta,surface}^{FW}(\omega) &= A_{\delta,surface}^{BW}(\omega) + A_{\delta,surface}^{SW}(\omega) \\ &= T_{\delta}(\omega) \cdot A_{\delta,bedrock}^{BW}(\omega) + A_{\delta,surface}^{SW}(\omega), \end{aligned} \quad (15.2)$$

where  $\delta = H, V$  means horizontal and vertical component, *BW* stands for body-waves, *SW* for surface-waves and  $T_{\delta}$  are the horizontal and vertical transfer functions. Equation (15.1) then gives

$$\begin{aligned} HV(\omega) &= \frac{T_H(\omega) \cdot A_{H,bedrock}^{BW}(\omega) + A_{H,surface}^{SW}(\omega)}{T_V(\omega) \cdot A_{V,bedrock}^{BW}(\omega) + A_{V,surface}^{SW}(\omega)} \\ &= \frac{A_{H,bedrock}^{BW}(\omega)}{A_{V,bedrock}^{BW}(\omega)} \cdot \frac{T_H(\omega) + \frac{A_{H,surface}^{SW}(\omega)}{A_{H,bedrock}^{BW}(\omega)}}{T_V(\omega) + \frac{A_{V,surface}^{SW}(\omega)}{A_{V,bedrock}^{BW}(\omega)}}, \end{aligned} \quad (15.3)$$

which the Author calls "quasi transfer spectrum" (QTS). Based on the hypothesis that the H/V spectral ratio at the bedrock is approximately unitary, *i.e.*,

$$A_{H,bedrock}^{BW}(\omega)/A_{V,bedrock}^{BW}(\omega) \simeq 1, \quad (15.4)$$

Eq. (15.3) shows that, when the surface-wave contribution is negligible, the function  $HV$  is close to  $T_H/T_V$ . As vertically incident body-waves are taken in account only, the P-wave and S-wave oscillation constitute respectively the vertical and horizontal ground-motion. In this theory, amplification in P-waves is not expected near the S-wave lower proper frequency, since P-wave velocity is supposed to be many times greater than the S-wave one, so the function  $HV$  should approximate the S-wave transfer function, around its peak frequency. If instead Rayleigh waves dominate, the function  $HV$  approximates the ratio  $A_{H,surface}^{SW}/A_{V,surface}^{SW}$ , whose peak frequency should, according to Nakamura, approximate the S-wave site resonance-frequency. Relying on other strong controversial assumptions (cf. Bard 1998), the Author concludes that the maximum of the function  $HV$ , hereafter called the H/V peak, represents the site S-wave lower resonance-frequency and the relative amplification factor, regardless of the Rayleigh-wave influence degree. The idea that the H/V peak only depend on S-wave resonance is reasserted in Nakamura (2008).

The one described above is, *de facto*, the first theoretical explanation of the H/V curve, whose the most important implication is probably that the peak frequency and amplitude of the function  $HV$  correspond to the S-wave resonance frequency and amplification factor of the site, respectively. Although this description is probably inadequate, it marked a turning point and made the fortune of the H/V technique. Indeed, while the statement about the amplitude has been proved to be almost always false, the correspondence between S-wave resonance and H/V-peak frequency has been always confirmed since then, in innumerable field experiments as well as by numerical simulations. This is by far the most useful and the most used feature of the H/V curve, but, surprisingly, it has not find a suitable complete theoretical explanation yet. Just in the particular case that surface waves are considered only (*vide infra*), the analytical formulae of Malischewsky and Scherbaum (2004) for the Rayleigh ellipticity demonstrate that the implication concerning the peak frequency is correct, in so far the impedance contrast is high enough. It is worth noting that Nakamura's theory explains the H/V curve just around its main peak frequency, and any extension to the whole H/V curve requests further assumptions (cf. Bard 1998).

Herak (2008) proposed a way to compute the H/V curve, which only involves vertically incident P and S waves. Like in first version of Nakamura's theory, no role is played by other seismic phases, included surface waves, but, differently from it, no *a priori* hypothesis is made about the P-wave site amplification. As Eq. 15.4 is supposed to hold at the bedrock, the H/V curve is given by

$$HV(\omega) \equiv \frac{A_{H,surface}^{BW}(\omega)}{A_{V,surface}^{BW}(\omega)} = \frac{AMP_S(\omega)}{AMP_P(\omega)}, \quad (15.5)$$

where  $A_{H,surface}^{BW}$  is given by the S-wave spectral amplitude and  $A_{V,surface}^{BW}$  is given by

the P-wave spectral amplitude, both computed at the Earth's free surface.  $AMP_P$  and  $AMP_S$  are the P-wave and S-wave amplification functions between the bedrock and the free surface, which are computed by the Herak's method, following Tsai (1970). Equation (15.5) shows that a direct estimation of the S-wave transfer function by the H/V is not always possible, because it is clear that  $HV(\omega) \simeq AMP_S(\omega)$  only if  $AMP_P(\omega) \simeq 1$  for all frequencies of interest. This approximation is valid only for relatively high Poisson's ratios, *i.e.*, when P-waves propagate through the topmost layers much faster than S-waves do, so that their resonance frequency is very higher than S-wave one (the Nakamura's hypothesis).

## 15.2.2 The Role of the Surface Waves

The fact that the H/V can be described in term of body waves travelling along particular patterns only is not at all obvious. In fact, the composition of ambient vibrations in term of the different seismic phases is not clearly understood till today, but all authors share the opinion that them are composed by all seismic phases travelling in the subsoil, although in not univocally defined proportions: the key and controversial aspect is the relative contribution of these seismic phases (see, *e.g.*, SESAME 2004). In fact, contrasting results exist both in field experiments and in numerical simulations, and it seems likely that the content in different seismic phases can drastically change in dependence on the subsoil stratigraphy and on sources' characteristics as well as in different frequency ranges.

So, as a sort of "counterparty" of the theories relied on body waves, theories based on surface-wave dominance have been developed. Already Nogoshi and Igarashi (1971) compare H/V curves from ambient vibrations with the ellipticity pattern of Rayleigh fundamental-mode, reckoning from the possibility of this comparison that this seismic phase plays the main role in the ambient vibrations. Subsequently, several other authors (*e.g.*, Lanchet and Bard 1994, 1995; Tokimatsu 1997; Konno and Ohmachi 1998; Wathelet et al. 2004) have been agreeing on the close relation existing between the H/V spectral ratio and the ellipticity of Rayleigh waves, which is reckoned as a consequence of their energetic predominance. In particular, Arai et al. (1996) and Tokimatsu (1997), like Nogoshi and Igarashi (1971), explain the ambient-vibration H/V curve by the ellipticity of the first mode of Rayleigh waves, and consider the feasibility of this explanation a suggestion of the surface-wave dominance. Surface-wave based is also the interpretation given by Konno and Ohmachi (1998), who point out that the H/V peak by ambient vibrations could be explained by the ellipticity of the fundamental Rayleigh mode as well as by the Airy phase of the fundamental Love mode, and also examine the role of the first higher Rayleigh mode. Moreover, in numerical simulations performed by these Authors, the H/V-peak amplitude roughly approximates the S-wave amplification factor, providing that a specific proportion between Rayleigh and Love waves exists; this mimics the Nakamura's statement, but in terms of surface waves instead that of body waves.

### ***15.2.3 The Sources' Role and the Full-Wavefield***

The above-mentioned theories give an explanation of the possible origin of the H/V curve, especially around its lower-frequency peak, but do not insert this explanation in a theory of the ambient-vibration wavefield. In other words, they say nothing about the origin of the H/V-curve overall shape, since they are not models for the ambient-vibration wavefield. In order to construct such a model, besides the composition of the ambient-vibration wavefield in terms of different seismic phases, another key element is its dependence on the subsoil properties. Without this piece of information, no possibility exists of using any experimental datum to estimate subsoil characteristics. For the models based on the hypothesis that just vertically incident P and S waves are important to describe the H/V curves, this aspect is simply exhausted by computing the propagation of these phases in a stratified model, as is the case of the above-mentioned Herak's approach. When the characteristics of free Rayleigh waves are needed, classical algorithms to compute them in a stratified medium can be applied. Besides these simple cases, some models have been developed in last couple of decades that manage this aspect by means of more detailed analysis of the ambient-vibration wavefield.

Lanchet and Bard (1994, 1995) consider that the ambient-vibration wavefield cannot be described in a deterministic way, because the greatest number of its sources are randomly located on the Earth's surface. So, they carry out a numerical simulation of the ambient-vibration wavefield by arranging a number of sources of different kinds acting in aleatory ways inside a given horizontal circle surrounding the receiver. For computational reasons, sources are located at depth of 2 m, while the receiver is on the Earth's surface. In this simulation, ambient-vibration displacement is the sum, in the time domain, of the ones produced by these sources in a fixed lapse of time and the H/V curve is the ratio between their horizontal and vertical Fourier amplitude-spectra. This is a purely numerical way to simulate the H/V curve, which has been used many times since then. By means of this model, Lanchet and Bard show the correspondence between the H/V peak-frequency and the S-wave resonance-frequency. Moreover, they also show that the H/V peak-frequency corresponds to the ellipticity peak-frequency of the Rayleigh fundamental mode as well as to the first-peak position of the ratio between horizontal and vertical ground-motion produced by S waves incident from a range of angles. Finally, they suggest that the overall shape of the H/V is determined by all seismic phases, and check that the peak amplitude, depending on many variables, does not correspond to the site amplification factor.

About in the same period, Field and Jacob (1993) propose a theoretical way to connect ambient-vibration displacement power-spectrum to the Green's function of the ground. They assume that the ambient vibrations are generated by an infinitude of uncorrelated point-like sources, uniformly located on the Earth's surface. The H/V curve in a point of the Earth's surface is obtained as the square root of the ratio between the horizontal and the vertical total power, computed, for any subsoil profile, as a finite sum of the contribution, in the frequency domain, given by the sources in a succession of annuli centred on the receiver and with increasing radii.

Differently from the Lanchet and Bard's model, which is purely numerical, this is an analytical model, although the sums have to be computed numerically. A decade later, Arai and Tokimatsu (2000, 2004) specialize this model to surface waves generated by sources with independent phases, which are approximated as continuously distributed on the Earth's surface. In this way, the total average spectral power is given by an integration on the horizontal plain, which can be carried out analytically. A source-free area around the receiver also exists in this model, with a radius equal to one wavelength of each propagation mode, in order to guarantee the surface-wave dominance and the possibility of describing these waves as plane waves. In order to make the power-integrals converging, these Authors insert an exponential damping factor originated by the "scattering" of the considered waves in the subsoil. A slightly modified version of this model was proposed by Lunedei and Albarello (2009), in which the damping originates by the material viscosity and the source-free area dimension does not more depend on each single propagation mode and can be done independent from the frequency too.

Fäh et al. (2001) use two ways to generate H/V synthetic curves. The first one is a numerical simulation made by a finite difference technique: these Authors agree that ambient-vibration sources are superficial, but they also introduce buried sources to describe scattering and wave conversion due to lateral heterogeneities. A large number of sources, with positions, depths and time-dependences chosen randomly, are distributed around a receiver. The second technique is a mode summation (Landisman et al. 1970). They particularly focus on the Rayleigh wave ellipticity of fundamental and higher modes, to explain the H/V-peak frequency, which they regard as the only trustworthy element, in that its amplitude and other features of the H/V curve also depend on other variables besides the S-wave velocity profile. Moreover, they identify stable parts of the H/V ratio, which are independent of the sources' distance and are dominated by the ellipticity of the fundamental Rayleigh mode, in the frequency band between the H/V-peak frequency, which they check to be close to the site S-wave fundamental resonance-frequency, and the first minimum of the H/V curve.

In their very important series of papers, Bonnefoy-Claudet et al. (2004, 2006, 2008) carry out a systematic study of the H/V curve by numerical simulations, in which the ambient vibrations are generated by a multitude of point-like forces, randomly oriented in the space and located relatively near to the observation point. They take advantage by a code developed by Hisada (1994, 1995) to compute the full displacement wavefield produced by these sources at some receivers, which are located on the Earth's surface. The total displacement at each receiver is computed by summing up, in the time domain, the one due to each sources. The H/V curve at each receiver is then computed as ratio between the average horizontal and the vertical Fourier-transform of this total displacement. In Bonnefoy-Claudet et al. (2006) the quasi-independence of the H/V curve from the specific sources' time-dependence has been confirmed. A dependency on the spatial horizontal distribution of near-surface sources as well as on the depth of buried sources has instead been observed, which however only slightly concerns the main-peak frequency. It instead shows relevant effects on H/V-peak amplitude and on the

appearance of secondary peaks. By using surface sources and several simple stratigraphical profiles, Bonnefoy-Claudet et al. (2008) check the good correspondence between the H/V-peak frequency and the S-wave resonance one. They also conclude that the H/V peak-frequency could be explained, depending on the stratigraphical situation, by Rayleigh ellipticity, Love Airy phase, S-wave resonance or a mix of them. In particular, the possibility of explaining the H/V main peak in term of Rayleigh ellipticity seems limited to profile with high impedance contrast (more than 4). An interesting result of this work is the coming out of the significant role of Love waves in the H/V curve and, more in general, in composing the ambient-vibration horizontal ground-motion. Moreover, the importance of taking into account all seismic phases propagating in the subsoil in constructing a suitable H/V model as well as the key role of the impedance contrast in controlling the origin of the H/V peak have been pointed out.

These pieces of work confirm that all seismic phases should be take into account to provide a reliable interpretation of the H/V curves. Then, the best way to reach an exhaustive description of the H/V curve by ambient vibrations seems the one firstly drawn by Field and Jacob (1993). In this line, Lunedei and Albarello (2010) extend their model, later denominated DSS (Distributed Surface Sources), to include all seismic phases. So, this model describes the full wavefield that composes the ambient vibrations, which are described as generated by a surface distribution of random sources. In this frame, the total average spectral-power is obtained by integrating the power given by the full Green's function relative to each sources and carried out by the above-mentioned Hisada's (1994, 1995) computer-program. Consequently, this model requires a double numerical integration: in the wavenumber and in the source/receiver distance. This model closely follows the Field and Jacob's (1993) one, the only relevant differences being in the relative weights between the horizontal and the vertical power, in taking into account the viscosity, and in the numerical code used to compute the Green's function. Both in full-wavefield and in surface-wave version of the DSS model, the H/V spectral ratio is obtained as square root of the ratio between the average spectral powers on the horizontal plane and along the vertical direction. By using these two versions of the DSS model, Albarello and Lunedei (2011) obtain some insights about the ambient-vibration wavefield structure. For a stratigraphical profile-set equal to the group M2\* in Table 15.1 (except for the damping values), characterized by a singular impedance contrast (*vide infra*), three frequency ranges are identified:

- Low-frequencies (below the S-wave resonance frequency,  $f_S$ ), where ambient-vibration spectral-powers are relatively low; in this range, the shallow layer acts as a high-pass filter, with an effect as more pronounced as sharper the impedance contrast is; both near sources and body waves dominate the wavefield; power spectra and H/V curves are significantly affected by source-free area dimension,  $V_P/V_S$  ratio and impedance-contrast strength at the bottom of the shallow layer;
- High-frequencies (above  $\max\{f_P, 2f_S\}$ , where  $f_P$  is the P-wave resonance frequency), where surface waves (both Love and Rayleigh, in their fundamental and higher modes) dominate the wavefield; in this range, spectral powers



**Table 15.1** Stratigraphical profiles used in the numerical experiments

M2					
$h$ (m)	$V_S$ (m/s)	$\nu$	$\rho$ (g/cm <sup>3</sup> )	$D_P$	$D_S$
25	200	0.333	1.9	0.001	0.001
5,000	1,000	0.333	2.5	0.001	0.001
$\infty$	2,000	0.257	2.5	0.001	0.001
M2*					
$h$ (m)	$V_S$ (m/s)	$\nu$	$\rho$ (g/cm <sup>3</sup> )	$D_P$	$D_S$
25	200	0.01–0.49	1.9	0.001	0.001
5,000	228–1,520	0.333	2.5	0.001	0.001
$\infty$	2,000	0.257	2.5	0.001	0.001
M3					
$h$ (m)	$V_S$ (m/s)	$V_P$ (m/s)	$\rho/\rho_4$	$D_P$	$D_S$
5	30	500	1	0.001	0.001
25	100	500	1	0.001	0.001
50	150	500	1	0.001	0.001
$\infty$	500	1,500	1	0.001	0.001

smoothly decrease with frequency as an effect of material damping, which also results in the fact that relatively near sources mostly contribute to ambient vibrations, as more as the frequency increases; H/V curves are almost unaffected by subsoil configuration and source/receiver distances;

- Intermediate frequencies, where the most of the ambient-vibration energy concentrates; in this range, sharp peaks in the horizontal and vertical spectral powers are revealed around its left and right bounds; irrespective of the subsoil structure and source-free area considered, horizontal ground motion is dominated by surface waves, with a varying combination of Love (in the fundamental mode) and Rayleigh waves that depends on the shallow-layer Poisson’s ratio (Love-wave contribution increases with it) and, to a minor extent, on the strength of the impedance contrast; in the vertical component, Rayleigh and other phases play different roles, both depending on the source-free area dimension and of  $V_P$  and  $V_S$  profiles.

In synthetic H/V curves produced by Albarello and Lunedei (2011), the peak frequency is generally very near to  $f_S$ , irrespective of the Poisson’s ratio and of the dimension of the source-free area. A weak sensitivity is revealed with respect to the impedance contrast only, and these findings enforce the common idea that the H/V peak-frequency is a good estimate of  $f_S$ . Amplitude and shape of the H/V curve around the peak appear instead more sensitive to subsoil and source configurations, and, in particular, no linear relationship results to exist between the H/V peak-amplitude and the impedance contrast, although, in general, this amplitude increases with the impedance contrast. Moreover, a significant dependence of the H/V-peak amplitude on the dimension of the source-free area (the amplitude tendentially increases with its dimension), on the shallow-layer Poisson’s ratio (the amplitude increases with it) and thickness (the amplitude decreases when the thickness increases) was obtained.

### 15.2.4 *A Different Point of View: The Diffuse Wavefield*

The model proposed more recently, named DFA (Diffuse Field Approach), significantly differs from the other ones, because it assumes that ambient vibrations constitute a diffuse wavefield. This means that seismic waves propagate in every (three-dimensional) spatial direction in a uniform and isotropic way and that a specific energetic proportion between P and S waves exists, which is the same whenever and wherever. This theory, initially developed in a full-space (Sánchez-Sesma and Campillo 2006), has been afterwards applied to an half-space and to a layered half-space (Sánchez-Sesma et al. 2011; Kawase et al. 2011). The link between the H/V curve and the subsoil configuration is simply given by the Green's function, computed for source and receiver located in the same position: its imaginary part, in the spectral domain, is proportional to the average spectral-power of the ambient-vibration ground-motion. A key element in the DFA theory, which is implied in the diffuse character of the wavefield, is the loss of any trace of the sources' characteristics, so no link between displacement and its sources is involved in this theory, *ergo*, no description of ambient-vibration sources is necessary. The model can describe the ambient-vibration full-wavefield as well as its surface-wave component only, depending on whether the full-wavefield Green's function or its surface-wave component is used.

### 15.2.5 *Current Research Branches*

In this relatively long history of the H/V spectral-ratio theory two alternative ways of thinking (cf., *e.g.*, Nakamura 2008) can be recognized: one that tries to explain the H/V features (and in particular its peak) as an effect of body-wave resonance and another that explains them by surface waves only. Although cumbersome under many points of view, theories that take in account the entire ambient-vibration wavefield can constitute the "pacifying" solution. Anyway, at present, surface-wave based theories keeps their interest, since relative computing is remarkably faster and surface-wave properties are more open to the analytical study, with respect the full-wavefield. As a consequence, apart from vertically incident models (which do not present news), the ambient-vibration H/V theoretical study has resulted nowadays in two research branches:

- The branch that studies the ambient-vibration wavefield as a whole; in this case, the theory aims to explain the H/V curve as it is measured in field, with all its components in terms of different seismic phases; this theory has to face the problems about the role of body and surface waves as well as about the role of the sources;

- The branch that should be better named “ellipticity theory” or “Rayleigh-wave H/V”; the subject is, in this case, just the Rayleigh ellipticity, both in theory and in experiments; as it chooses, *a priori*, to take into account the Rayleigh ellipticity only, the relative theory does not need to deal neither with body waves nor with the wavefield sources, while experiments are devoted to extract Rayleigh waves from the recorded signal (*e.g.*, Fäh et al. 2001).

In order to avoid misinterpretations, it is important to distinguish the complete H/V curve from the Rayleigh ellipticity curve.

Currently, the first theory is essentially represented by models that consider surface sources, in all possible variants (the purely numerical one or the semi-analytical DSS) and the DFA: in next section a comparison between the DSS and the DFA is summarized, while in the subsequent a mention to new developments in these models is done. Afterwards, a section is devoted to the ellipticity theory.

### 15.3 Comparison Between the DSS and the DFA Models

In last years, some conference notes (García-Jerez et al. 2011, 2012a, b, c) were presented to compare the most recent two models of the H/V spectral ratio: the Distributed Surface Sources (DSS) and the Diffuse Field Approach (DFA). Each of them is a complete theory of the ambient vibrations and has solid theoretical foundations. Through this section, which summarizes the salient elements of these comparisons,  $G_{ij}(\mathbf{x}_A, \mathbf{x}_B, \omega)$  is the frequency-domain displacement Green’s function for the considered Earth’s model at the point  $\mathbf{x}_A$  on the free surface along the  $i$ -th Cartesian axis due to a point-like force located at the point  $\mathbf{x}_B$  and directed along the  $j$ -th Cartesian axis. The three Cartesian spatial directions are marked by subscripts 1, 2 (for the horizontal plane) and 3 (for the vertical direction), while  $r$  and  $\theta$  are the polar coordinates on the horizontal plane.

#### 15.3.1 The DSS Model

The DSS model assumes that the ambient vibrations are generated by a *continuum* of aleatory point-like sources distributed on the Earth’s free-surface. The ground motion that they produce propagates to the receiver without significant scattering, except the one due to the stratigraphical interfaces present in the layered subsoil (impedance contrasts). This model has been formulated under the assumption of weakly dissipative medium, for both ambient-vibration full-wavefield (Lunedei and Albarello 2010) and surface-wave component only (Lunedei and Albarello 2009). For the full-wavefield, ambient-vibration powers along the three spatial Cartesian directions are:

$$P_1(\omega) + P_2(\omega) = \pi\sigma^2 \int_{r_{\min}}^{\infty} \left[ (\sigma_1^2 + \sigma_2^2) \left( |G_{11}(0, 0, 0; r, 0, 0; \omega)|^2 + |G_{22}(0, 0, 0; r, 0, 0; \omega)|^2 \right) + 2\sigma_3^2 |G_{13}(0, 0, 0; r, 0, 0; \omega)|^2 \right] r dr, \quad (15.6)$$

$$P_3(\omega) = \pi\sigma^2 \int_{r_{\min}}^{\infty} \left[ (\sigma_1^2 + \sigma_2^2) |G_{31}(0, 0, 0; r, 0, 0; \omega)|^2 + 2\sigma_3^2 |G_{33}(0, 0, 0; r, 0, 0; \omega)|^2 \right] r dr, \quad (15.7)$$

where the arguments of the Green's function are expressed in Cylindrical coordinates  $(r, \theta, x_3)$ ,  $\sigma^2$  stands for the total surface variance-density of the random sources and  $\sigma_j^2$  for its relative component along the  $j$ -th Cartesian axis. Formulae in Eqs. (15.6) and (15.7) correct the weight given by Field and Jacob (1993) to the vertical-load Green's functions.  $r_{\min} \geq 0$  is the radius of the circular free-source area surrounding the receiver. Finally, the H/V spectral ratio is calculated as

$$HV(\omega) \equiv \sqrt{\frac{P_1(\omega) + P_2(\omega)}{P_3(\omega)}}. \quad (15.8)$$

In the case of predominance of surface waves, expressions in Eqs. (15.6) and (15.7) assume a simpler form. Compact formulae were first given by Arai and Tokimatsu (2004) for an elastic stratified medium, under some additional simplifying hypotheses (asymptotic long-distance forms of the Green's functions, suitable source-free areas, incoherent summation of modal contributions):

$$P_1(\omega) + P_2(\omega) = \frac{\kappa}{2}\sigma^2 \left\{ \sum_{m \in \text{RAYLEIGH}} [2\sigma_3^2 + \chi_m^2(\sigma_1^2 + \sigma_2^2)] \left( \frac{A_{Rm}}{k_{Rm}} \right)^2 \chi_m^2 + \sum_{m \in \text{LOVE}} (\sigma_1^2 + \sigma_2^2) \left( \frac{A_{Lm}}{k_{Lm}} \right)^2 \right\}, \quad (15.9)$$

$$P_3(\omega) = \frac{\kappa}{2}\sigma^2 \sum_{m \in \text{RAYLEIGH}} [2\sigma_3^2 + \chi_m^2(\sigma_1^2 + \sigma_2^2)] \left( \frac{A_{Rm}}{k_{Rm}} \right)^2, \quad (15.10)$$

where  $A_{Rm}$  and  $A_{Lm}$  represent the medium response of Rayleigh and Love waves for the  $m$ -th mode (Harkrider 1964) and  $\chi_m$  is the corresponding Rayleigh wave ellipticity (as a real quantity), while  $\kappa$  is a frequency independent damping parameter, representative of the "scattering" effect. Under the same simplifying hypotheses, Lunedei and Albarello (2009) proposed a different implementation, which includes the effects of material damping (viscosity):

$$P_1(\omega) + P_2(\omega) = \frac{\sigma^2}{4} \sum_{m \in \text{RAYLEIGH}} [2\sigma_3^2 + \chi_m^2(\sigma_1^2 + \sigma_2^2)] \chi_m^2 \frac{(A_{Rm})^2}{k_{Rm} \alpha_{Rm}} \exp(-2\alpha_{Rm} r_{\min}) + \frac{\sigma^2}{4} \sum_{m \in \text{LOVE}} \frac{(A_{Lm})^2}{k_{Lm} \alpha_{Lm}} \exp(-2\alpha_{Lm} r_{\min}) \quad (15.11)$$

$$P_3(\omega) = \frac{\sigma^2}{4} \sum_{m \in \text{RAYLEIGH}} [2\sigma_3^2 + \chi_m^2(\sigma_1^2 + \sigma_2^2)] \frac{(A_{Rm})^2}{k_{Rm} \alpha_{Rm}} \exp(-2\alpha_{Rm} r_{\min}), \quad (15.12)$$

where  $\alpha_{Lm}$  and  $\alpha_{Rm}$  are the attenuation factors for the  $m$ -th Love and Rayleigh mode respectively, which depend on the viscous properties of the medium. These formulae explicitly depend on the source-free area radius  $r_{\min} \geq 0$ , which can be set either constant or frequency dependent.

### 15.3.2 The DFA Model

The DFA model assumes that the relative power of each seismic phase is prescribed by the energy equipartition principle. Under this hypothesis, proportionality exists between the Fourier-transformed autocorrelation (power spectrum), at any point of the medium, and the imaginary part of the Green's function computed when source location corresponds to the one of the receiver (Sánchez-Sesma et al. 2011). The assumption of a major role of multiple scattering involving all possible wavelengths is behind this formulation.

In this model, under the assumption of a pure 1D configuration (horizontal layering), where the horizontal directions are indistinguishable, the H/V spectral ratio is given as

$$HV(\omega) \equiv \sqrt{\frac{P_1(\omega) + P_2(\omega)}{P_3(\omega)}} = \sqrt{\frac{2\text{Im}[G_{11}(\mathbf{x}; \mathbf{x}; \omega)]}{\text{Im}[G_{33}(\mathbf{x}; \mathbf{x}; \omega)]}}, \quad (15.13)$$

where  $P_j(\omega) \propto \text{Im}[G_{jj}(\mathbf{x}; \mathbf{x}; \omega)]$  for  $j = 1, 2, 3$ ,  $\mathbf{x}$  is an arbitrary point on the free surface and “Im” means imaginary part. Equation (15.13) links the function  $HV$  with the subsoil mechanical properties, and accounts for the contributions of surface and body waves.

Whenever surface waves can be considered to represent the dominant contribution to the wavefield, the model can be simplified by rewriting the Green's functions in terms of their well-known modal characteristic, so the powers can be expressed as

$$P_1(\omega) = P_2(\omega) \propto -\text{Im}[G_{11}(\mathbf{x}; \mathbf{x}; \omega)] \rightarrow \frac{1}{4} \sum_m \{A_{Rm} \chi_m^2 + A_{Lm}\}, \quad (15.14)$$

$$P_3(\omega) \propto -\text{Im}[G_{33}(\mathbf{x}; \mathbf{x}; \omega)] \rightarrow \frac{1}{2} \sum_m A_{Rm}. \quad (15.15)$$

### 15.3.3 Comparison

The differences between DSS and DFA model are shown in a more explicit form if their versions for surface waves are compared (Eqs. 15.9, 15.10 or 15.11, 15.12 vs 15.14, 15.15). The formulae have a similar structure, but the contributions of each wave-type and mode to the total power differ. Indeed, they depend on  $A_{\bullet m}$  in the DFA formulation and on  $\left(\frac{A_{\bullet m}}{k_{\bullet m}}\right)^2$  or  $\frac{(A_{\bullet m})^2}{k_{\bullet m} \alpha_{\bullet m}} \cdot \exp(-2\alpha_{\bullet m} x_{\min})$  in the DSS one, where “ $\bullet$ ” indicates Love or Rayleigh waves. The square operator in the last model is a consequence of the power computation; in the DFA model, the correct physical dimension is guaranteed by an appropriate factor that multiplies the imaginary part of the Green’s function. So, while in the DSS the energy repartition among contributing waves depends on the energy of each wave (expressed by its square amplitude), in the DFA this repartition is established by the Green’s function for coincident source and receiver. This is a very important physical difference between the two models. The common inverse wavenumber  $1/k_{\bullet m}$  in the DSS formulae represents an effect of the long-range wave propagation from the generic source to the receiver, while the other  $1/k_{\bullet m}$  factor or the correspondent  $1/\alpha_{\bullet m}$  is the effect of the integration on the horizontal distance to compute the total source distribution effect. Both these elements are obviously absent in the DFA. In both the considered models, the function  $HV$  restricted to surface-waves tends to the ellipticity of (non-dispersive) Rayleigh waves over a half-space and depend on the characteristics of the deeper medium, as  $\omega \rightarrow 0$ .

In order to study the differences and similarities of these two models, a set of synthetic tests was performed (see notes quoted at the beginning of the section): results relative to stratigraphic profiles listed in Table 15.1 are here shown. The group of profiles M2\* is generated by varying the profile M2, and all these profiles basically consist of a layer overlying an half-space (although a intermediate thick buffer layer exists, which prevents from sharply unrealistic truncation of surface-wave higher modes in the range of frequency of interest). The profile M3, instead, presents two major and a weak impedance contrasts. For the DSS model,  $\sigma_1^2 = \sigma_2^2 = \sigma_3^2 = 1/3$  was set.

Albarelo and Lunedei (2011) find, for the profile M2, significant contributions of body waves for frequencies around and below the S-wave resonance frequency  $f_s$  (2 Hz in this case), and a clear surface-wave dominance for frequencies larger than the P-wave one  $f_p$  (4 Hz in this case). This fact reflects on the deviation between blue (full wavefield, FW) and green (surface waves, SW) curves in Fig. 15.1a around the peak frequency. When a circular source-free area with a radius of 10 m exists (Fig. 15.1b), the FW produces an H/V peak equal to the one of the SW,

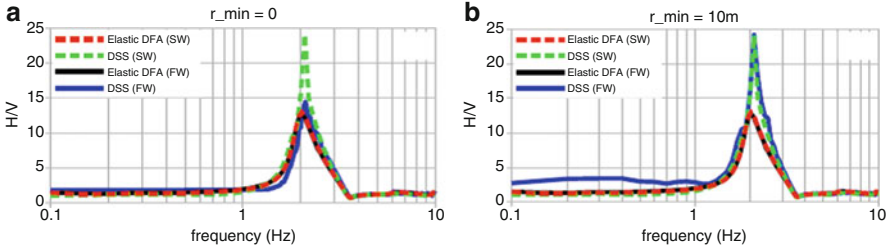


**Fig. 15.1** H/V curves for the stratigraphy M2 obtained by the DSS for the full-wavefield (blue) and the surface-wave component (green), as well as by the DFA for the full-wavefield (black) and the surface-wave component (red); (a) no source-free area is considered; (b) a source-free area with radius 10 m is set in the DSS

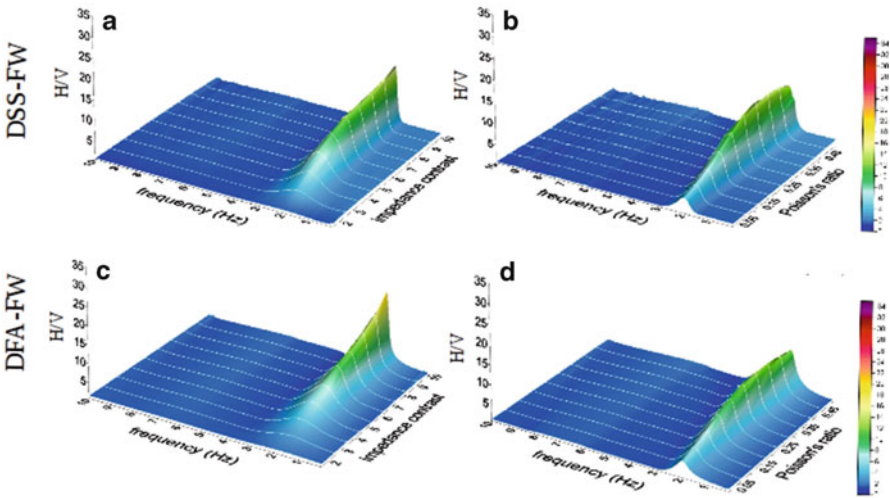


**Fig. 15.2** Upper panels: H/V curves computed by the full-wavefield DSS for models in set M2\*, with  $r_{min}=0$ . Lower panels: respective counterparts obtained by using the full-wavefield DFA

probably as a consequence of the more efficient propagation of these last at long distances. The elastic DFA results show no difference between FW and SW H/V-curve, which peak amplitude is less than the DSS one.

Moreover, as said in the previous section, a parametric study of this stratigraphy is realized by considering the profiles' family M2\*, which full-wavefield results are shown in Fig. 15.2.

By using the profile M3, which presents two important impedance contrasts at 5 and 80 m and a minor one at 30 m depth, it has been pointed out that, differently from the single-layer case, remarkable differences in the H/V shape deduced from DFA and DSS can occur for more complicated subsoil structures. Rough calculations from the S-wave travel-time lead to expected resonance frequencies of 1.5 and 0.33 Hz respectively for the principal contrasts and 0.6 for the secondary one. Two

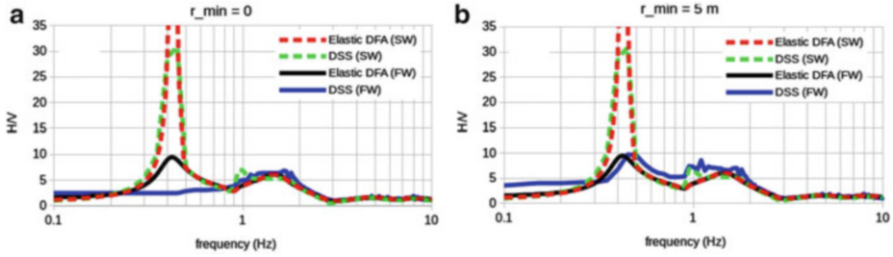


**Fig. 15.3** H/V curves from DFA and DSS method for the profile M3; (a) sources are allowed on the whole Earth's surface; (b) near sources are removed from around the receiver up to the distance of 5 m

peaks appear in the elastic DFA computation near to 0.4 and 1.5 Hz (which can be associated with the two subsoil principal interfaces), both for the FW (black lines in Fig. 15.3) and the SW (red lines in Fig. 15.3). The DSS response is more complex. When no source-free area exists, the DSS-FW H/V (blue line in Fig. 15.3a) only shows the peak correspondent to the shallowest impedance contrast, while the other is retrieved by the DSS-SW counterpart (green line in Fig. 15.3a). The main peak is recovered in the DSS-FW H/V curve if close sources are removed from the calculations, as Fig. 15.3b (blue line) shows for  $r_{\min} = 5$  m, and in that case the overall shape of the DFA-FW and DSS-FW curves approximately approach. These results suggest that DFA and DSS might lead to closer results whenever a suitable source-free area is used in the DSS-FW computations, letting surface waves play a predominant role. The SW results seem very similar in every case.

The results obtained indicate that both the DSS and the DFA provide reasonable full-wavefield and surface-wave synthetics of H/V spectral ratios. In spite of the rather different underlying hypotheses, DFA and DSS lead to similar H/V curves for stratigraphic profiles with a dominant impedance contrast (M2\*). Relative H/V main peaks match the first S-wave resonance frequency ( $f_S$ ) in a very good way. Nevertheless, peak amplitudes may differ and show non-trivial dependence on impedance contrast and Poisson's ratio. Results relative to DSS also depend on the source distribution around the receiver. For both models, surface waves represent the dominant contribution at high enough frequencies, whereas body waves play an important role around and below  $f_S$ . For a stratigraphy with more impedance contrasts, some variability occurs in the overall shape of the H/V curve in the full-wavefield DSS when sources are present or absent near the receiver. Whenever near sources are eliminated from the DSS computation (so surface waves are playing the major role), both DFA and DSS provide very similar results, and this seems suggest that, although physical bases are different, surface-wave behaviour described by DFA and DSS is very similar. In any case, the differences in the overall H/V curve features make clear that further investigations on the relationships between DFA and DSS are still necessary.



## 15.4 A Mention to the Most Recent Results in H/V Modelling

To overcome some limits of the full-wavefield DSS model, a new version of it has been very recently proposed by Lunedei and Albarello (2014, 2015). This new theory bases on describing the ambient-vibration ground-motion displacement and its generating force fields as three-variate, three-dimensional stochastic processes stationary both in time and space. In this frame, the displacement power can be linked with the source filed power *via* the Green's function, which, in turn, depends on the subsoil configuration.

About the DFA model, very recently García-Jerez et al. (2013) have shown some consequence, at low and high frequencies, of its application to a simple crustal model. The most recent development of this model is its application to a case where a lateral variation exists, by Matsushima et al. (2014).

Finally, the DSS model gives a suitable base to compare the different definitions of the H/V curve appeared in literature. Called  $H_N$  and  $H_E$  the spectra of the ambient-vibration ground-motion horizontal components along two orthogonal directions, Albarello and Lunedei (2013) compare the following definitions for the merging of these horizontal components:

1. No combination, that is, two H/V curves are computed by considering separately the two directions,
2. Arithmetic mean,  $H \equiv (H_N + H_E)/2$ ,
3. Geometric mean,  $H \equiv \sqrt{H_N \cdot H_E}$ ,
4. Vector summation,  $H \equiv \sqrt{H_N^2 + H_E^2}$ ,
5. Quadratic mean,  $H \equiv \sqrt{(H_N^2 + H_E^2)/2}$ ,
6. Maximum horizontal value,  $H \equiv \max\{H_N, H_E\}$ ,

and, given  $L$  elements of the statistical sample (typically, time-windows), the two ways to experimentally define the H/V ratio:

- (a) The square root of the ratio between the arithmetic mean of the spectral powers on the  $L$  time-windows,
- (b) The arithmetic mean of the H/V ratios computed in each of the  $L$  time-windows.

It results that the H/V estimates are biased of 46 % to more than 100 % and that, while the definition (a) quickly reduces its bias-size (for all cases 1–6) as  $L$  increases, this does not happen for the definition (b). Figure 15.4 shows the bias pattern when the number of degree of freedom ( $m=2L$ ) increases. A role of the smoothing procedures in reducing the bias also emerges in the quoted paper.

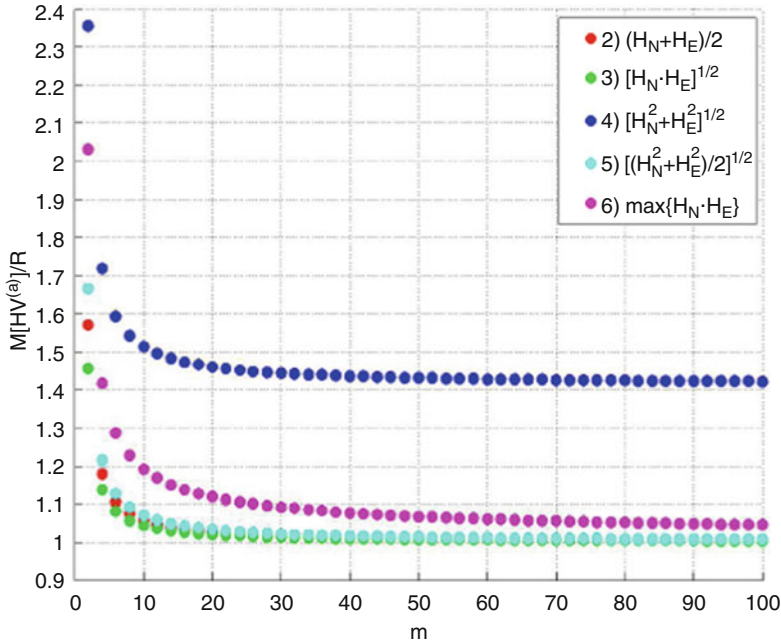


**Fig. 15.4** Relative bias of the different H/V definitions with respect the mathematical expectations of H/V (named R)

## 15.5 Rayleigh Ellipticity Theory

In this research branch, the H/V curve is identified *a priori* and by definition with the ellipticity of Rayleigh waves, which is the subject of the study. A short summary on this topic can be found, *e.g.*, in SESAME (2004). Moreover, a part of the popular Geopsy software (<http://www.geopsy.org/>) is focused on the ellipticity. Fäh et al. (2001) propose a way to extract Rayleigh ellipticity experimentally and to compare it with a theoretical model. Malischewsky and Scherbaum (2004) investigate some important properties of H/V on the basis of Rayleigh waves by re-analysing an old formula of Love, and obtaining essential results to apply the H/V method. Later, the theory for the ellipticity of Rayleigh waves was carefully studied by Tran (2009) and Tran et al. (2011) with particular regard to applications for the H/V method.

### 15.5.1 Osculation Points

An interesting special and less-known feature of the ellipticity is the role of so-called osculation points, which are those points (see, *e.g.*, Forbriger 2003) where two dispersion curves of surface waves (especially Rayleigh waves) come

very near to each other and eventually even cross under certain circumstances (see Kausel et al. 2015). For sake of simplicity, just a stratigraphic profile constituted by a single horizontal layer over an half-space (LOH) is used to describe the special behaviour of the ellipticity at these points. Named  $h$  and  $V_{S1}$  the shallow-layer thickness and S-wave velocity respectively,  $V_{S2}$  the S-wave velocity of the half-space,  $r_d$  the ratio between their densities and  $r_S \equiv V_{S1}/V_{S2}$ , the only impedance contrast of the profile is  $r_S \cdot r_d$ . Dimensionless surface-wave phase-velocity  $C = c/V_{S1}$  and frequency  $\bar{f} \equiv \frac{h}{V_{S1}} \cdot f$  are also defined. The limit case of this model is the model LFB (layer with fixed bottom), defined by the limit  $r_S \rightarrow 0$ . Some analytical formulae exist for the LFB model, but for the LOH model there are approximate formulae only. Usually it is assumed, for the LOH model, that the Rayleigh-wave H/V (ellipticity) curve has, as a function of the frequency, one peak depending on the subsoil properties, whereas a model with two layers over a half-space may have two peaks (e.g., Wathelet et al. 2004). However, a more careful theoretical analysis shows that also a LOH model exhibits two peaks within a certain parameter range. Tran (2009) establishes that two peaks emerge for the LFB model when the Poisson's ratio  $\nu_1$  of the shallow layer is in the interval  $\nu_1^{(1)} < \nu_1 < \nu_1^{(2)}$ , with  $\nu_1^{(2)} = 0.25$  and  $\nu_1^{(1)} \approx 0.2026$ , which last is a solution of the equation

$$1 - 2\sqrt{\gamma} \sin\left(\frac{\pi}{2}\sqrt{\gamma}\right) = 0, \quad (15.16)$$

with  $\gamma \equiv \frac{1-2\nu_1}{2(1-\nu_1)} = \frac{V_{S1}^2}{V_{S2}^2 \rho_1}$ . The first peak of the Rayleigh-wave H/V curve (i.e., in this frame, the Rayleigh ellipticity curve) is for  $\bar{f}_1 = 0.25$ , while the second peak occurs for

$$\bar{f}_2 = \frac{C}{2\pi\sqrt{C^2\gamma - 1}} \cdot \arccos\sqrt{\frac{\gamma(1 - C^2) + C^2/4}{\gamma(1 - C^2) + 1}}, \quad (15.17)$$

and  $C$  is the solution of the transcendental equation

$$\begin{aligned} & \sqrt{C^2 - 1} \cdot \arccos\sqrt{\frac{\gamma(1 - C^2) + C^2/4}{\gamma(1 - C^2) + 1}} \\ &= \sqrt{C^2\gamma - 1} \cdot \arccos\left[\frac{2}{2 - C^2} \cdot \sqrt{\frac{\gamma(1 - C^2) + C^2/4}{\gamma(1 - C^2) + 1}}\right]. \end{aligned} \quad (15.18)$$

At the osculation point, which for the LFB occurs at  $\nu_1^{(2)}$  and is a degeneration point, the H/V curve changes its properties from having two peaks to having one peak and one zero-point. A similar behaviour is exhibited for the LOH model:

- if  $\bar{\nu}_1^{(1)} < \nu_1 < \bar{\nu}_1^{(2)}$  the H/V curve has two peaks,
- if  $\bar{\nu}_1^{(2)} < \nu_1 < 0.5$  the H/V curve has one peak and one zero-point,

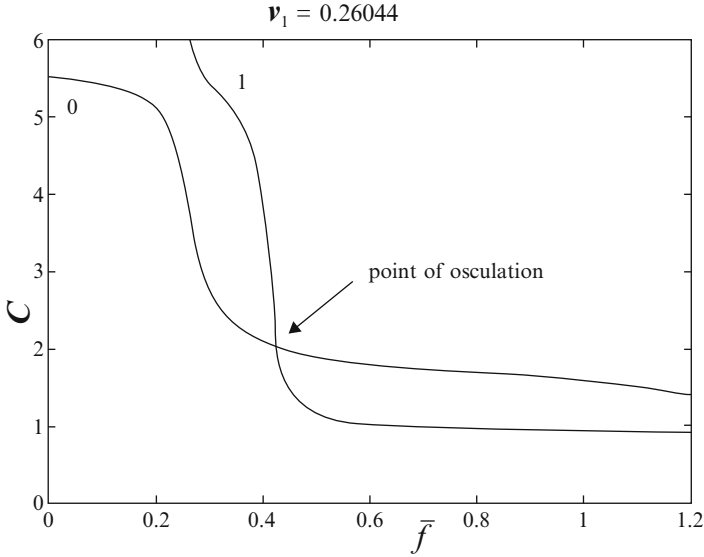


**Fig. 15.5** Dimensionless dispersion curves  $C(\bar{f})$  for the fundamental ( $0$ ) and first higher ( $1$ ) Rayleigh mode for a LOH model with parameters  $r_s = 1/6$ ,  $r_d = 2/2.7$ ,  $\nu_1 = 0.26044$ ,  $\nu_2 = 0.2506$ , where  $\nu_1$  and  $\nu_2$  are the Poisson’s ratios of the shallow layer and the half-space, respectively (After Tran 2009)

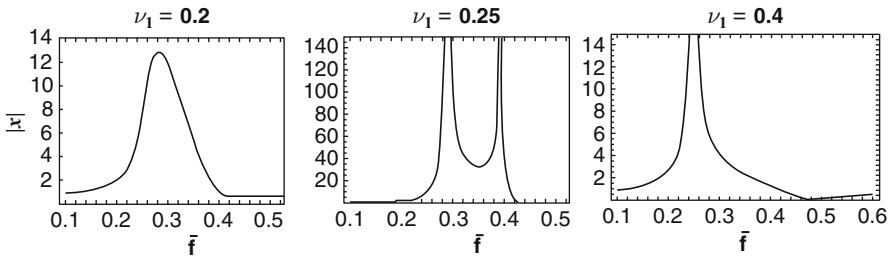


**Fig. 15.6** Behaviour of H/V curve for the fundamental mode for different shallow-layer Poisson’s ratios. *Left*:  $\nu_1 = 0.2$  (one maximum, *i.e.*, one peak with finite amplitude); *middle*:  $\nu_1 = 0.25$  (2 peaks); *right*:  $\nu_1 = 0.4$  (one peak and one zero-point)

where  $\bar{\nu}_1^{(1)}$  and  $\bar{\nu}_1^{(2)}$  are complicated functions of the model parameters; in particular,  $\bar{\nu}_1^{(2)}$  is the value at which the osculation point occurs, whose an example is shown in Fig. 15.5. The first peak occurs nearby  $\bar{f} = 0.25$  when  $r_s$  is small enough (Malischewsky and Scherbaum 2004).

The behaviour of the H/V given by the Rayleigh ellipticity  $\bar{\chi}$  in dependence on  $\bar{f}$  for the LOH model with parameters of Fig. 15.5 and different  $\nu_1$  values is presented in Fig. 15.6. The critical values  $\bar{\nu}_1^{(1)}$  and  $\bar{\nu}_1^{(2)}$  are, in this case,  $\bar{\nu}_1^{(1)} = 0.24319$  and  $\bar{\nu}_1^{(2)} = 0.26044$ .

It turns out that the osculation point is, for LOH again, the point where the H/V curve changes its behaviour dramatically. The practical consequences of this behaviour are discussed for models in Israel and Mexico in Malischewsky et al. (2010).

## 15.6 Conclusions

This short *excursus* on the way to construct a theory able to explain the H/V curve features shows that, in spite of the strongly different hypothesis underlying the various proposed theories, the key element of the H/V curve, *i.e.*, the main peak frequency, is reproduced in a more than acceptable way by all of them. Even though, in order to be able to profoundly understand the relative role of the model and of the stratigraphy in affecting the synthetic H/V curves, a big systematic comparative work would be necessary, the capability of different theories of giving realistic features of this quantity reinforces the idea that the H/V curve, and in particular its main peak frequency, express intrinsic properties of the subsoil, *i.e.*, that it is eminently determined by the stratigraphical profile, *ergo* it gives a true piece of information about the subsoil seismic properties. By a phrase, the H/V seems to resist theories!

**Acknowledgments** Authors are grateful to Prof. Dario Albarello for useful suggestions about the subject of this paper.

**Open Access** This chapter is distributed under the terms of the Creative Commons Attribution Noncommercial License, which permits any noncommercial use, distribution, and reproduction in any medium, provided the original author(s) and source are credited.

## References

- Albarello D, Lunedei E (2011) Structure of an ambient vibration wavefield in the frequency range of engineering interest ([0.5, 20] Hz): insights from numerical modelling. *Near Surface Geophys* 9:543–559. doi:[10.3997/1873-0604.2011017](https://doi.org/10.3997/1873-0604.2011017)
- Albarello D, Lunedei E (2013) Combining horizontal ambient vibration components for H/V spectral ratio estimates. *Geophys J Int* 194:936–951. doi:[10.1093/gji/ggt130](https://doi.org/10.1093/gji/ggt130)
- Arai H, Tokimatsu K, Abe A (1996) Comparison of local amplifications estimated from microtremor f-k spectrum analysis with earthquake records. In: Proceedings of the 11th world conferences on earthquake engineering (WCEE), Acapulco. <http://www.nicee.org/wcee/>
- Arai H, Tokimatsu K (2000) Effect of Rayleigh and Love waves on microtremor H/V spectra. In: Proceedings of the 12th world conferences on earthquake engineering (WCEE), Auckland. <http://www.nicee.org/wcee/>
- Arai H, Tokimatsu K (2004) S-wave velocity profiling by inversion of microtremor H/V spectrum. *Bull Seismol Soc Am* 94(1):53–63

- Bard PY (1998) Microtremor measurements: a tool for site effect estimation? In: Proceedings of the 2nd international symposium on the effects of surface geology on seismic motion, Yokohama, pp 1251–1279
- Bonnefoy-Claudet S, Cornou C, Kristek J, Ohrnberger M, Wathelet M, Bard PY, Moczo P, Fäh D, Cotton F (2004) Simulation of seismic ambient noise: I. Results of H/V and array techniques on canonical models. In: Proceedings of the 13th world conferences on earthquake engineering (WCEE), Vancouver. <http://www.nicee.org/wcee/>
- Bonnefoy-Claudet S, Cornou C, Bard PY, Cotton F, Moczo P, Kristek J, Fäh D (2006) H/V ratio: a tool for site effects evaluation. Results from 1-D noise simulation. *Geophys J Int* 167:827–837. doi:[10.1111/j.1365-246X.2006.03154.x](https://doi.org/10.1111/j.1365-246X.2006.03154.x)
- Bonnefoy-Claudet S, Köhler A, Cornou C, Wathelet M, Bard PY (2008) Effects of Love waves on microtremor H/V ratio. *Bull Seismol Soc Am* 98(1):288–300. doi:[10.1785/0120070063](https://doi.org/10.1785/0120070063)
- Fäh D, Kind F, Giardini D (2001) A theoretical investigation of average H/V ratios. *Geophys J Int* 145:535–549
- Field E, Jacob K (1993) The theoretical response of sedimentary layers to ambient seismic noise. *Geophys Res Lett* 20(24):2925–2928
- Forbriger T (2003) Inversion of shallow-seismic wavefields: I. Wavefield transformation. *Geophys J Int* 153:735–752
- García-Jerez A, Luzón F, Sánchez-Sesma FJ, Santoyo MA, Albarello D, Lunedei E, Campillo M, Iturrarán-Viveros U (2011) Comparison between two methods for forward calculation of ambient noise H/V spectral ratios. AGU Fall Meeting 2011, 5–9 Dec 2011, San Francisco. <http://abstractsearch.agu.org/meetings/2011/FM/sections/S/sessions/S23A/abstracts/S23A-2230.html>
- García-Jerez A, Luzón F, Albarello D, Lunedei E, Sánchez-Sesma FJ, Santoyo MA (2012a) Comparison between ambient vibration H/V synthetics obtained from the Diffuse Field Approach and from the Distributed Surface Load method. In: Proceedings of the XXIII general assembly of the European seismological commission (ESC 2012), 25–30 Aug 2012, Moscow, pp 412–413
- García-Jerez A, Luzón F, Albarello D, Lunedei E, Santoyo MA, Margerin L, Sánchez-Sesma FJ (2012b) Comparison between ambient vibrations H/V obtained from the diffuse field and distributed surface source models. In: Proceedings of the 15th world conferences on earthquake engineering (WCEE), 24–28 Sept 2012, Lisbon. <http://www.nicee.org/wcee/>
- García-Jerez A, Luzón F, Lunedei E, Albarello D, Santoyo MA, Margerin L, Sánchez-Sesma FJ (2012c) Confronto fra le curve H/V da vibrazioni ambientali prodotte dai modelli di distribuzione superficiale di sorgenti e di campo diffuso, Atti del XXXI Convegno Nazionale del Gruppo Nazionale di Geofisica della Terra Solida, 20–22 Nov 2012, Potenza, pp 148–157. <http://www2.ogs.trieste.it/gngts/> (Sessione 2, Tema 2) (in Italian)
- García-Jerez A, Luzón F, Sánchez-Sesma FJ, Lunedei E, Albarello D, Santoyo MA, Almendros J (2013) Diffuse elastic wavefield within a simple crustal model. Some consequences for low and high frequencies. *J Geophys Res* 118:1–19. doi:[10.1002/2013JB010107](https://doi.org/10.1002/2013JB010107)
- Harkrider DG (1964) Surface waves in multilayered elastic media. Part 1. *Bull Seismol Soc Am* 54:627–679
- Herak M (2008) ModelHVSR – a Matlab® tool to model horizontal-to-vertical spectral ratio of ambient noise. *Comput Geosci* 34(11):1514–1526. doi:[10.1016/j.cageo.2007.07.009](https://doi.org/10.1016/j.cageo.2007.07.009)
- Hisada Y (1994) An efficient method for computing Green's functions for a layered half-space with sources and receivers at close depths. *Bull Seismol Soc Am* 84(5):1456–1472
- Hisada Y (1995) An efficient method for computing Green's functions for a layered half-space with sources and receivers at close depths (part 2). *Bull Seismol Soc Am* 85(4):1080–1093
- Kanai K, Tanaka T (1961) On microtremors. VIII. *Bull Earthq Res Inst* 39:97–114
- Kausel E, Malischewsky P, Barbosa J (2015) Osculations of spectral lines in a layered medium. *Wave Motion* (in press). doi:[10.1016/j.wavemoti.2015.01.004](https://doi.org/10.1016/j.wavemoti.2015.01.004), (<http://dx.doi.org/10.1016/j.wavemoti.2015.01.004>)
- Kawase H, Sánchez-Sesma FJ, Matsushima S (2011) The optimal use of horizontal-to-vertical spectral ratios of earthquake motions for velocity inversions based on diffuse-field theory for plane waves. *Bull Seismol Soc Am* 101(5):2001–2014. doi:[10.1785/0120100263](https://doi.org/10.1785/0120100263)

- Konno K, Ohmachi T (1998) Ground-motion characteristics estimated from spectral ratio between horizontal and vertical components of microtremors. *Bull Seismol Soc Am* 88(1):228–241
- Lanchet C, Bard PY (1994) Numerical and theoretical investigations on the possibilities and limitations of Nakamura's technique. *J Phys Earth* 42:377–397
- Lanchet C, Bard PY (1995) Theoretical investigations on the Nakamura's technique. In: Proceedings of the 3rd international conference on recent advanced in geotechnical earthquake engineering and soil dynamics, 2–7 Apr 1995, St. Louis (Missouri), vol II
- Landisman L, Usami T, Sato Y, Massè R (1970) Contributions of theoretical seismograms to the study of modes, rays, and the earth. *Rev Geophys Space Phys* 8(3):533–589
- Lunedei E, Albarello D (2009) On the seismic noise wavefield in a weakly dissipative layered Earth. *Geophys J Int* 177:1001–1014. doi:[10.1111/j.1365-246X.2008.04062.x](https://doi.org/10.1111/j.1365-246X.2008.04062.x) (Erratum: *Geophys J Int* 179:670. doi:[10.1111/j.1365-246X.2009.04344.x](https://doi.org/10.1111/j.1365-246X.2009.04344.x))
- Lunedei E, Albarello D (2010) Theoretical HVSR curves from full wavefield modelling of ambient vibrations in a weakly dissipative layered Earth. *Geophys J Int* 181:1093–1108. doi:[10.1111/j.1365-246X.2010.04560.x](https://doi.org/10.1111/j.1365-246X.2010.04560.x) (Erratum: *Geophys J Int* 192:1342. doi:[10.1093/gji/ggs047](https://doi.org/10.1093/gji/ggs047))
- Lunedei E, Albarello D (2014) Complete wavefield modelling of ambient vibrations from a distribution of correlated aleatory surface sources: computation of HVSR. Special Session “Ambient Noise for soil and building studies” of the Second European Conference on Earthquake Engineering and Seismology (2ECEES), 24–29 Aug 2014, Istanbul
- Lunedei E, Albarello D (2015) Horizontal-to-vertical spectral ratios from a full-wavefield model of ambient vibrations generated by a distribution of spatially correlated surface sources. *Geophys J Int* 201:1140–1153. doi:[10.1093/gji/ggv046](https://doi.org/10.1093/gji/ggv046)
- Malischewsky PG, Scherbaum F (2004) Love's formula and H/V-ratio (ellipticity) of Rayleigh waves. *Wave Motion* 40:57–67
- Malischewsky PG, Zaslavsky Y, Gorstein M, Pinsky V, Tran TT, Scherbaum F, Flores Estrella H (2010) Some new theoretical considerations about the ellipticity of Rayleigh waves in the light of site-effect studies in Israel and Mexico. *Geofisica Int* 49:141–151
- Matsushima S, Hirokawa T, De Martin F, Kawase H, Sánchez-Sesma FJ (2014) The effect of lateral heterogeneity on horizontal-to-vertical spectral ratio of microtremors inferred from observation and synthetics. *Bull Seismol Soc Am* 104(1):381–393. doi:[10.1785/0120120321](https://doi.org/10.1785/0120120321)
- Nakamura Y, Ueno M (1986) A simple estimation method of dynamic characteristics of subsoil. In: Proceedings of the 7th Japan earthquake engineering symposium, Tokyo, pp 265–270 (in Japanese)
- Nakamura Y (1989) A method for dynamic characteristics estimation of subsurface using microtremor on the ground surface. *Q Rep Railw Tech Res Inst* 30(1):25–30
- Nakamura Y (2000) Clear identification of fundamental idea of Nakamura's technique and its applications. In: Proceedings of the 12th world conference on earthquake engineering (WCEE), Auckland. <http://www.nicce.org/wcee/>
- Nakamura Y (2008) On the H/V spectrum. In: Proceedings of the 14th world conference on earthquake engineering (WCEE), Beijing. <http://www.nicce.org/wcee/>
- Nogoshi M, Igarashi T (1971) On the amplitude characteristics of microtremor (part 2). *J Seismol Soc Jpn* 24:26–40 (in Japanese with English abstract)
- Sánchez-Sesma FJ, Campillo M (2006) Retrieval of the Green's function from cross correlation: the canonical elastic problem. *Bull Seismol Soc Am* 96(3):1182–1191. doi:[10.1785/0120050181](https://doi.org/10.1785/0120050181)
- Sánchez-Sesma FJ, Rodríguez M, Iturrarán-Viveros U, Luzón F, Campillo M, Margerin L, García-Jerez A, Suarez M, Santoyo MA, Rodríguez-Castellanos A (2011) A theory for microtremor H/V spectral ratio: application for a layered medium. *Geophys J Int* 186:221–225
- SESAME (2004) European Research Project, WP12–deliverable D23.12. Guidelines for the implementation of the H/V spectral ratio technique on ambient vibrations: measurements, processing and interpretation (see Bard PY et al (2004) The SESAME Project: an overview and main results. In: 13th world conference on earthquake engineering (WCEE), Vancouver, 1–6 Aug 2004, paper no. 2207, <http://www.nicce.org/wcee/>)

- Tokimatsu K (1997) Geotechnical site characterization using surface waves. In: Ishihara K (ed) *Earthquake geotechnical engineering: proceedings of IS-Tokyo '95, the first international conference on earthquake geotechnical engineering*, Tokyo, 14–16 Nov 1995, vol 3. A A Balkema Publishers, Rotterdam, pp 1333–1368
- Tsai NC (1970) A note on the steady-state response of an elastic half-space. *Bull Seismol Soc Am* 60:795–808
- Tran TT (2009) The ellipticity (H/V-ratio) of Rayleigh surface waves. PhD dissertation, Friedrich-Schiller-University, Jena
- Tuan TT, Scherbaum F, Malischewsky PG (2011) On the relationship of peaks and troughs of the ellipticity (H/V) of Rayleigh waves and the transmission response of single layer over half-space models. *Geophys J Int* 184:793–800
- Wathelet M, Jongmans D, Ohrnberger M (2004) Surface-wave inversion using a direct search algorithm and its application to ambient vibration measurements. *Near Surface Geophys* 2:211–221